Electronic Supplementary Material (ESI) for RSC Advances.

Supporting Information

Synthesis, Structure and Magnetic properties of $(Eu_{1-x}Mn_x)MnO_{3-\delta}$

Jianming Deng[b], Aimei Yang[b], M. A. Farid[a], Hao. Zhang[a], Jian Li[a], Hongxing Zhang[a] Guobao Li[a], Laijun Liu[b]*, Junliang Sun[a], and Jianhua Lin[a]**

[a]Beijing National Laboratory for Molecular Sciences, State Key Laboratory of Rare Earth Materials Chemistry and Applications, College of Chemistry and Molecular Engineering, Peking University, Beijing 100871, P. R. China

[b]College of Materials Science and Engineering, Guilin University of Technology, Guilin 541004, P. R. China

Email: liguobao@pku.edu.cn, and jhlin@pku.edu.cn; Tel: (8610)62750342, Fax: (8610)62753541.

Contents

1. The refinement details of the X-ray diffraction data for M1 to M7

The Powder X-ray powder diffraction data collected at room temperature for M1 to M7 are refined using GSAS software. The refinement details listed in Table S1 and S2. The corresponding Rietveld plots are shown in Figure S1, S2, …, S8.

Table S1 Rietveld refinement details of the X-ray diffraction data for M1, M2, M3 and M4 in *Pnma*

	M1	M2	M3	M4
Lattice parameter (Å)	a=5.8522(2), b=7.4580(3), c=5.3481(2)	a=5.8323(2), b=7.4610(3), c=5.3448(2)	a=5.8122(2), b=7.4647(2), c=5.3415(2)	a=5.7891(2), b=7.4700(3), c=5.3389(2)
Atom	x, y, z	x, y, z	x, y, z	x, y, z
Eu/Mn[a]	0.0783(2), 0.2500, 0.9820(3)	0.0768(2), 0.2500, 0.9826(3)	0.0768(2), 0.2500, 0.9819(3)	0.0746(2), 0.2500, 0.9825(2)
Mn	0.0000, 0.0000, 0.5000	0.0000, 0.0000, 0.5000	0.0000, 0.0000, 0.5000	0.0000, 0.0000, 0.5000
O1	0.4876(3), 0.2500, 0.0892(3)	0.4814(3), 0.2500, 0.0920(2)	0.4801(2), 0.2500, 0.0936(3)	0.4710(2), 0.2500, 0.0968(3)
O2	0.3183(2), 0.0385(2), 0.7146(3)	0.3247(2), 0.0406(2), 0.7205(3)	0.3297(2), 0.0394(2), 0.7188(2)	0.3268(2), 0.0455(3), 0.7246(3)
R factor[b]	R_{wp}=0.021, R_p=0.012	R_{wp}=0.020, R_p=0.011	R_{wp}=0.019, R_p=0.011	R_{wp}=0.019,R_p=0.010

[a]The occupancy of Eu/Mn is 1.000/0.000 for M1, 0.975/0.025 for M2, 0.950/0.050 for M3, 0.925/0.075 for M4.
[b]R_p is sum($|I_0-I_C|$)/sum(I_0), and R_{wp} is weighted R factors for X-ray diffraction data.

Table S2 Rietveld refinement details of the X-ray diffraction data for M5, M6 and M7

	M5	M6	M7
Phase 1	$Eu_{1-x}Mn_xMnO_3$	$Eu_{1-x}Mn_xMnO_3$	$Eu_{1-x}Mn_xMnO_3$
Lattice parameter (Å)	a=5.7625(2), b=7.4740(3), c=5.3359(2)	a=5.7391(2), b=7.4791(3), c=5.3328(2)	a=5.7405(2), b=7.4786(3), c=5.3321(2)
Space group	*Pnma*	*Pnma*	*Pnma*
Atom	x, y, z	x, y, z	x, y, z
Eu/Mn	0.0714(2), 0.2500, 0.9837(2)	0.0710(2), 0.2500, 0.9838(2)	0.0713(2), 0.2500, 0.9855(2)
Mn	0.0000, 0.0000, 0.5000	0.0000, 0.0000, 0.5000	0.0000, 0.0000, 0.5000
O1	0.4679(2), 0.2500, 0.1125(2)	0.4929(2), 0.2500, 0.1264(2)	0.4739(2), 0.2500, 0.1136(2)
O2	0.3351(2), 0.0442 (1), 0.7341(2)	0.3155(2), 0.0451(1), 0.7220(2)	0.3195(3), 0.0460(2), 0.7176(3)
Phase 2			Mn_3O_4
Lattice parameter (Å)			a=5.7649(1), c=9.4860(1)
Space group			*I* 4_1/*a m d*
Atom			x, y, z
Mn1			0.0000, 0.2500, 0.8750
Mn2			0.0000, 0.5000, 0.5000
O			0.0000, 0.4746 (1), 0.2627(1)
R factor[e]	R_{wp}=0.019,R_p=0.010	R_{wp}=0.021,R_p=0.012	R_{wp}=0.023,R_p=0.013

[a]The occupancy of Eu/Mn is 0.900/0.100 for M5, 0.875/0.125 for M6, 0.874/0.126 for M7.

[b]R_p is sum($|I_0-I_C|$)/sum(I_0), and R_{wp} is weighted R factors for X-ray diffraction data.

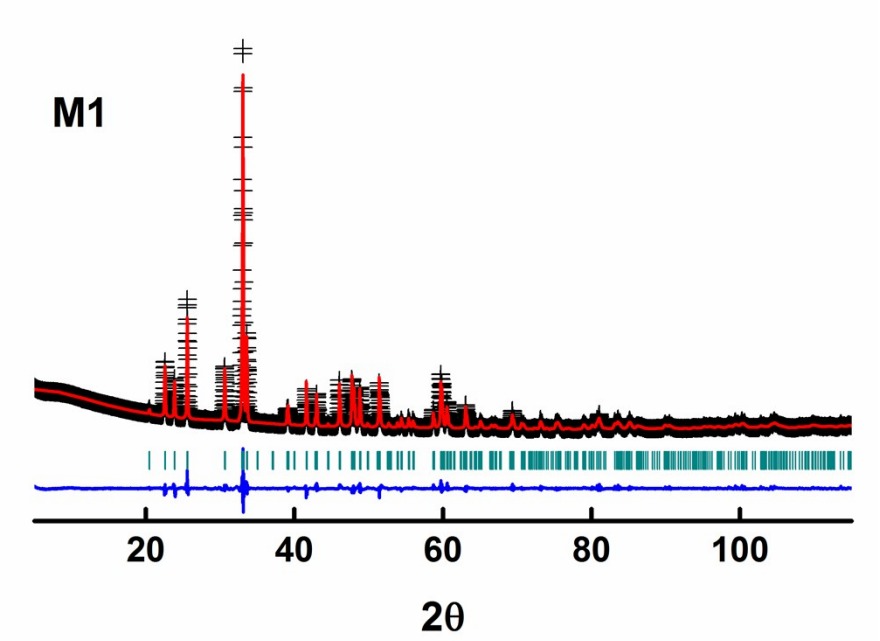

Figure S1 Rietveld plots of powder X-ray diffraction patterns (λ_1=1.5405 Å and λ_2=1.5443 Å) for M1 at room temperature. The symbol + represents the observed value, the solid line represents the calculated value; the marks below the diffraction patterns are the calculated reflection positions, and the difference curve is shown at the bottom of the figure.

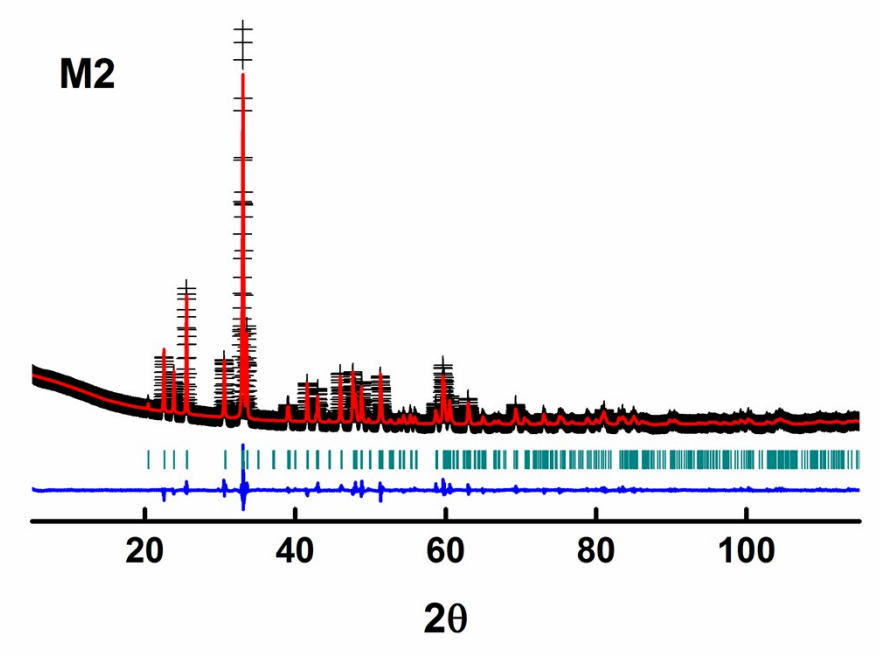

Figure S2 Rietveld plots of powder X-ray diffraction patterns (λ_1=1.5405 Å and λ_2=1.5443 Å) for M2 at room temperature. The symbol + represents the observed value, the solid line represents the calculated value; the marks below the diffraction patterns are the calculated reflection positions, and the difference curve is shown at the bottom of the figure.

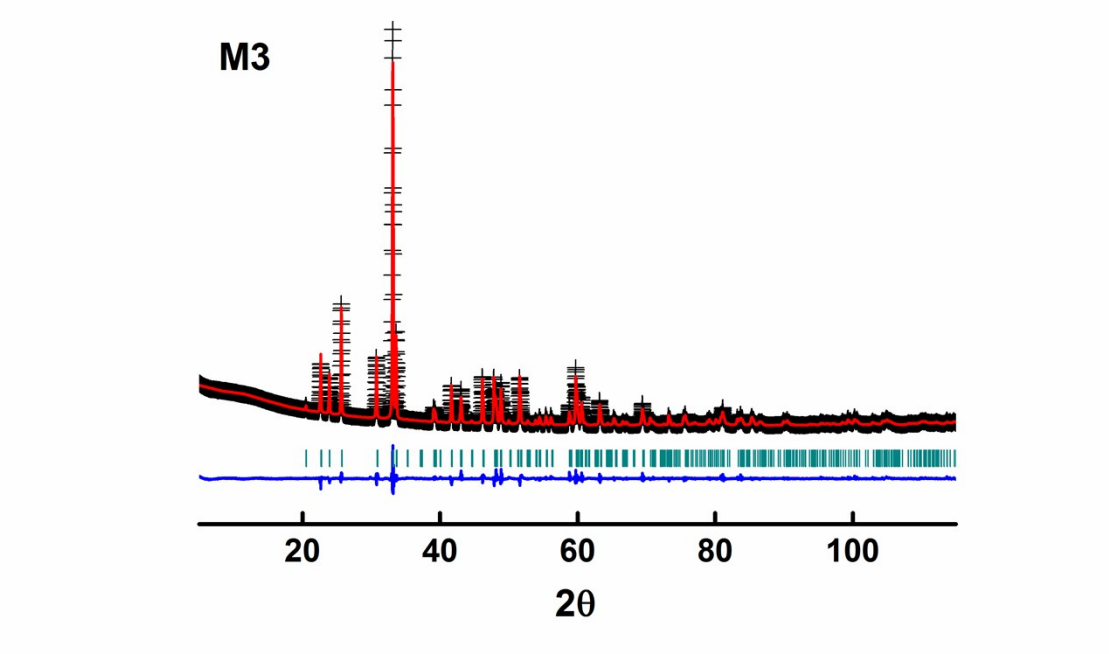

Figure S3 Rietveld plots of powder X-ray diffraction patterns (λ_1=1.5405 Å and λ_2=1.5443 Å) for M3 at room temperature. The symbol + represents the observed value, the solid line represents the calculated value; the marks below the diffraction patterns are the calculated reflection positions, and the difference curve is shown at the bottom of the figure.

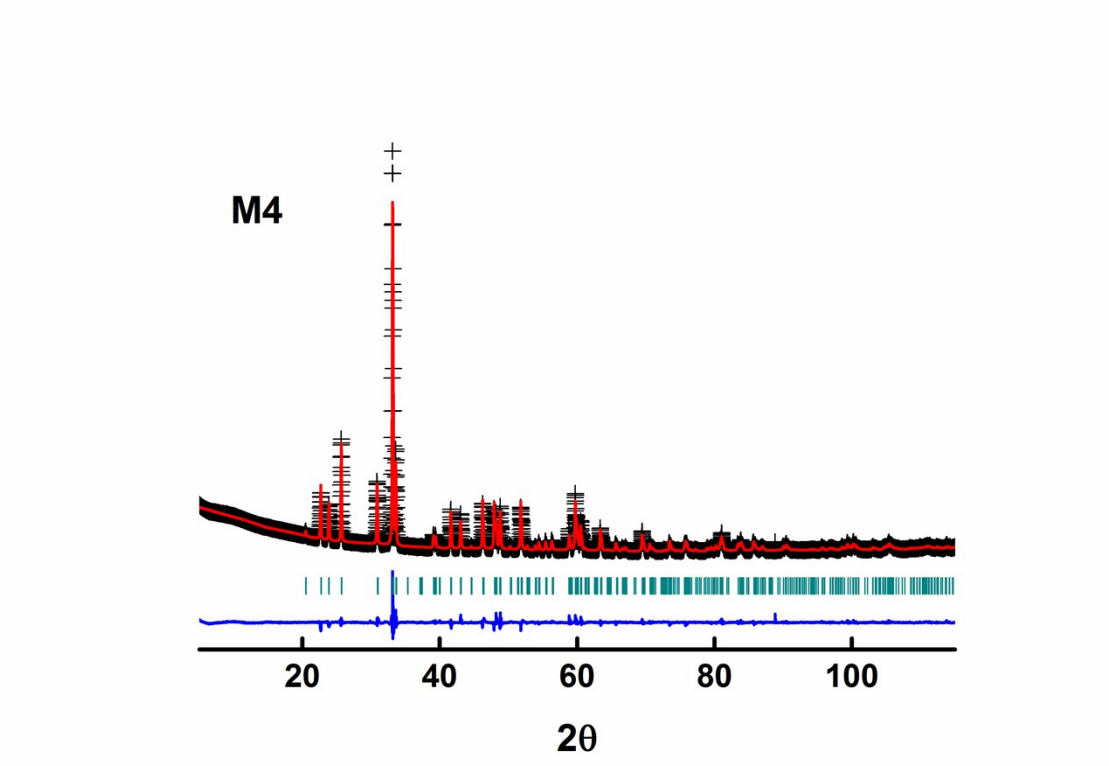

Figure S4 Rietveld plots of powder X-ray diffraction patterns (λ_1=1.5405 Å and λ_2=1.5443 Å) for M4 at room temperature. The symbol + represents the observed value, the solid line represents the calculated value; the marks below the diffraction patterns are the calculated reflection positions, and the difference curve is shown at the bottom of the figure.

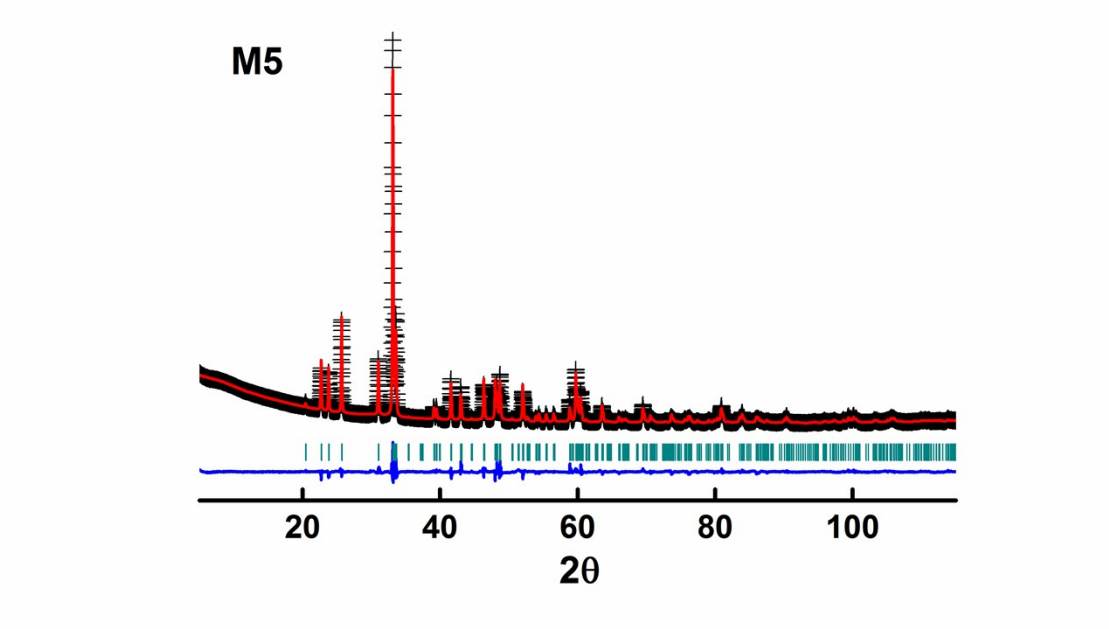

Figure S5. Rietveld plots of the X-ray diffraction data for M5 around room temperature. The symbol + represents the observed value, the solid line represents the calculated value, the marks below the diffraction patterns are the calculated reflection positions, and the difference curve is shown at the bottom of the figure.

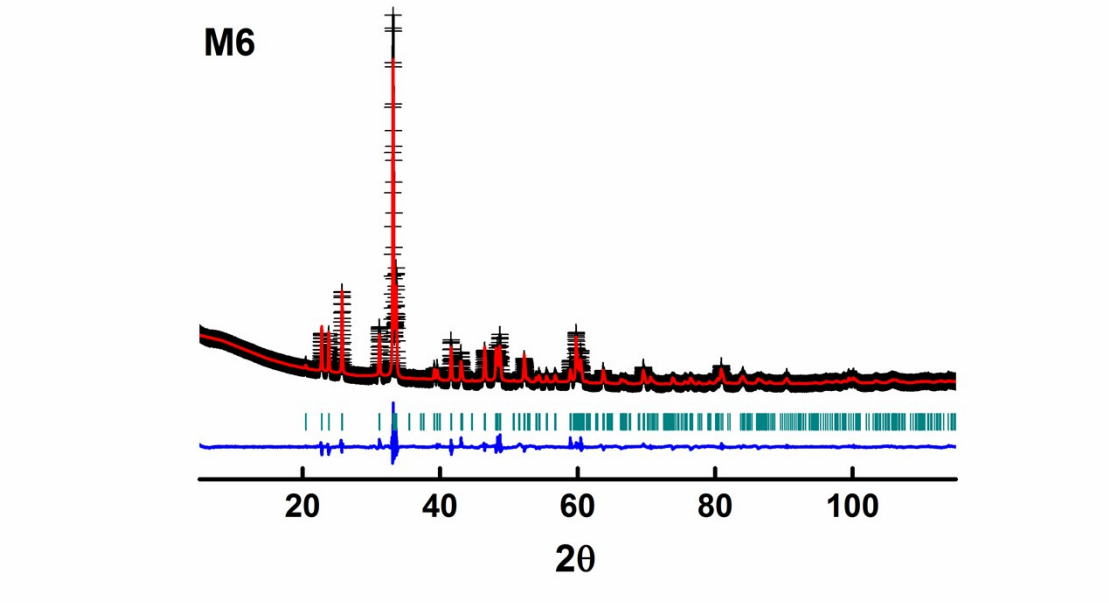

Figure S6 Rietveld plots of the X-ray diffraction data for M6 around room temperature. The symbol + represents the observed value, the solid line represents the calculated value, the marks below the diffraction patterns are the calculated reflection positions, and the difference curve is shown at the bottom of the figure.

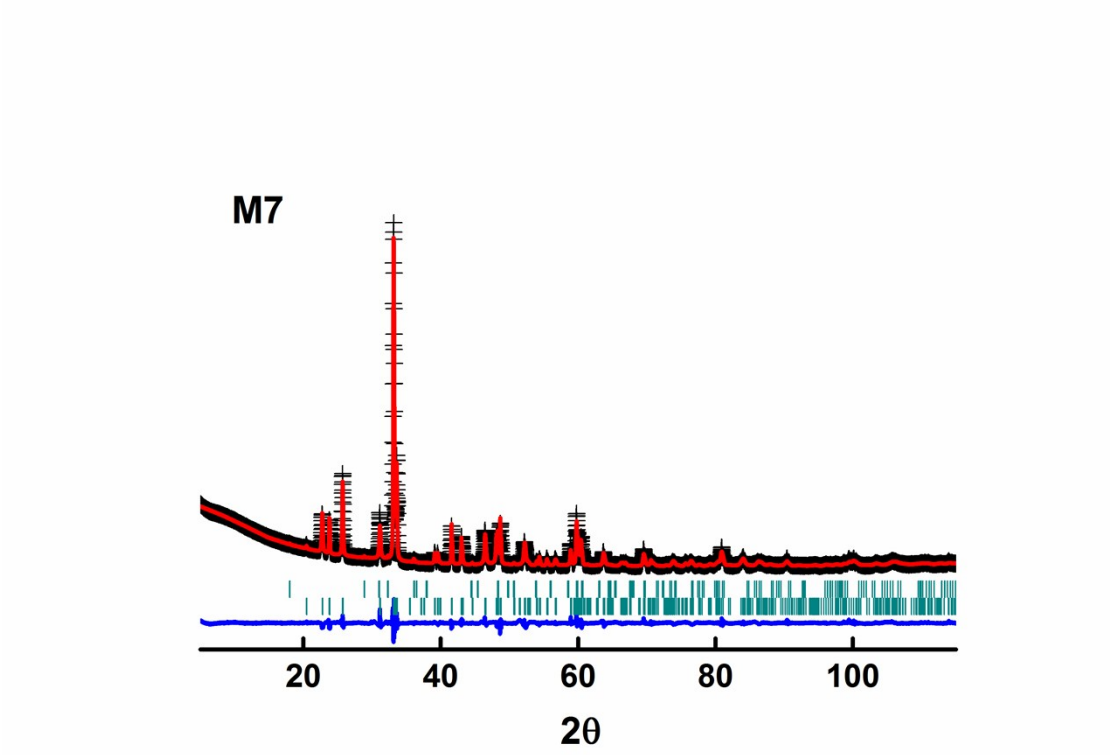

Figure S7 Rietveld plots of powder X-ray diffraction patterns (λ_1=1.5405 Å and λ_2=1.5443 Å) for M8 at room temperature. The symbol + represents the observed value, the solid line represents the calculated value; the marks below the diffraction patterns are the calculated reflection positions for $(Eu_{1-x}Mn_x)MnO_{3-\delta}$ (the second line (from upper to low)), Mn_3O_4 (the first line), and the difference curve is shown at the bottom of the figure.

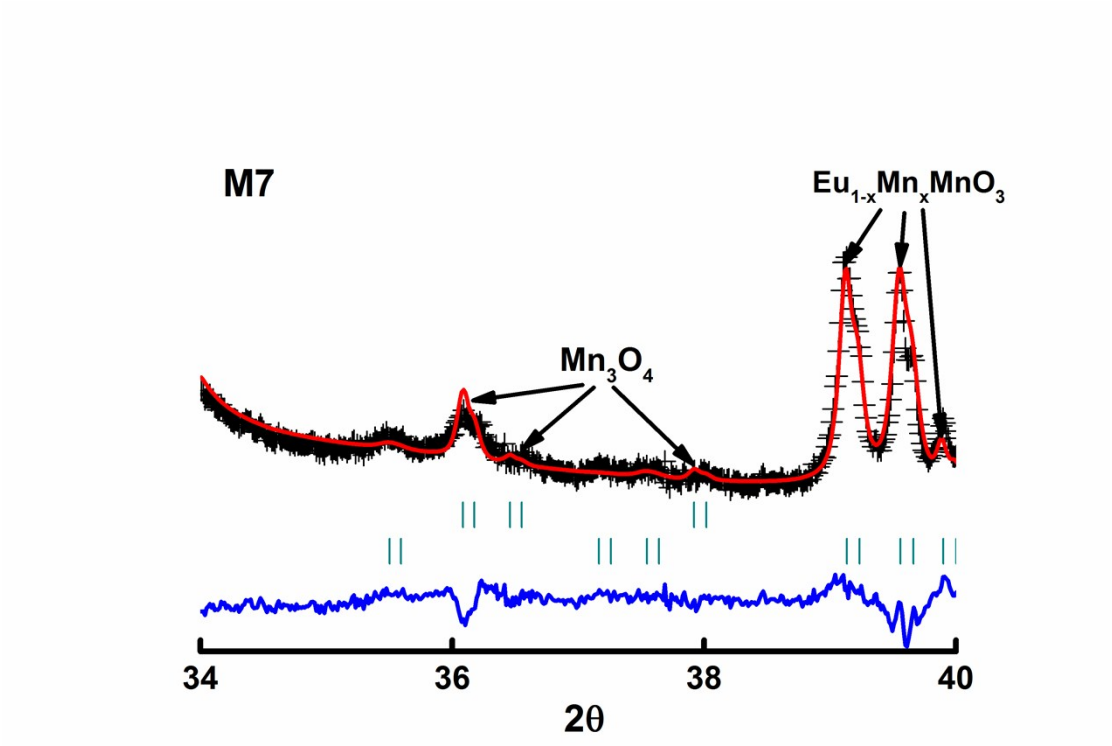

Figure S8 Enlarged figure of Figure S8. The symbol + represents the observed value, the solid line represents the calculated value; the marks below the diffraction patterns are the calculated reflection positions for $(Eu_{1-x}Mn_x)MnO_{3-\delta}$ (the second line (from upper to low)), Mn_3O_4 (the first line), and the

difference curve is shown at the bottom of the figure.

2. Temperature dependence magnetization of M2 to M6

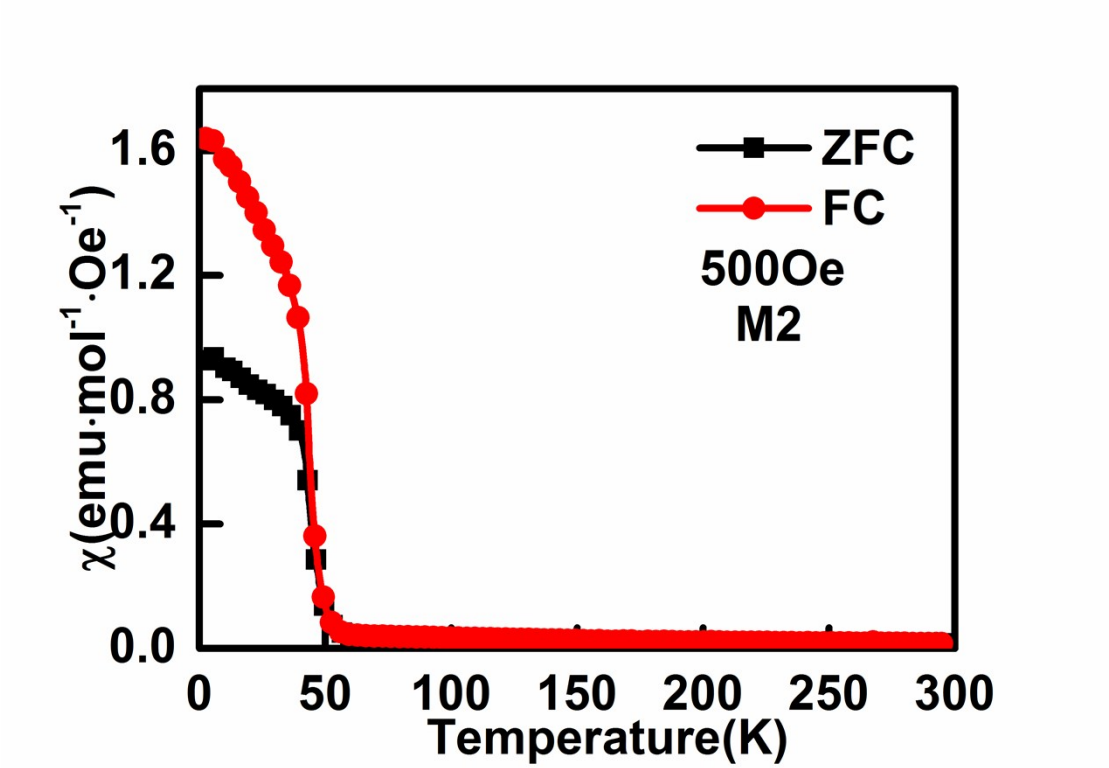

Figure S9 Temperature dependence magnetization of the samples M2 under 500 Oe in ZFC (zero field cooling) and FC modes.

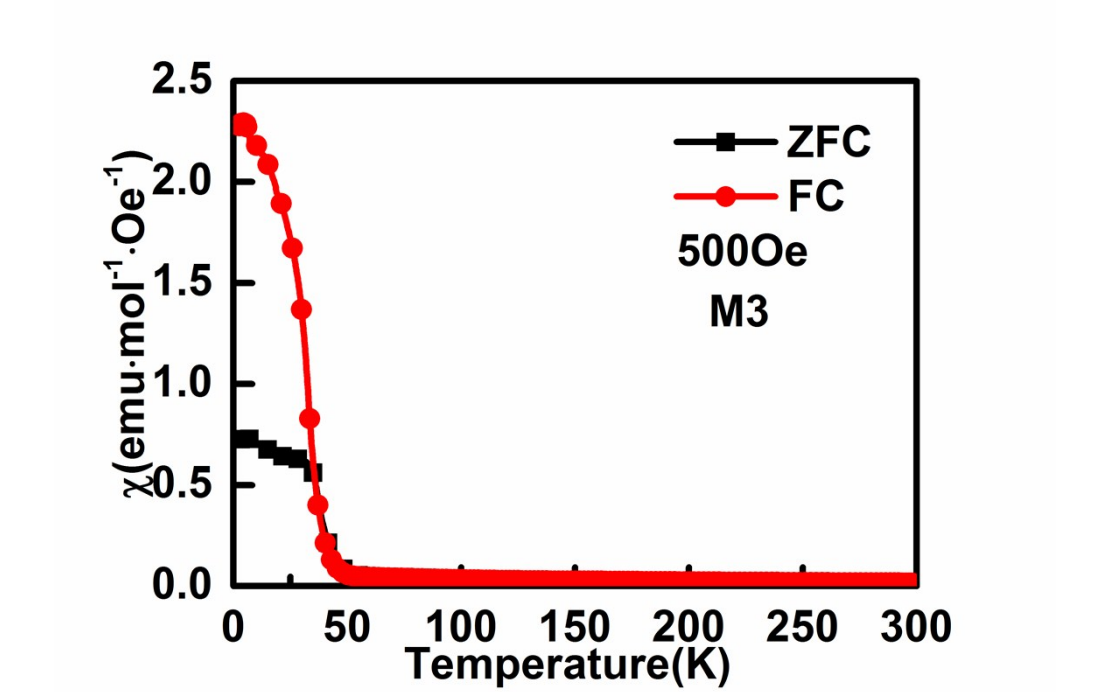

Figure S10 Temperature dependence magnetization of the samples M3 under 500 Oe in ZFC (zero field cooling) and FC modes.

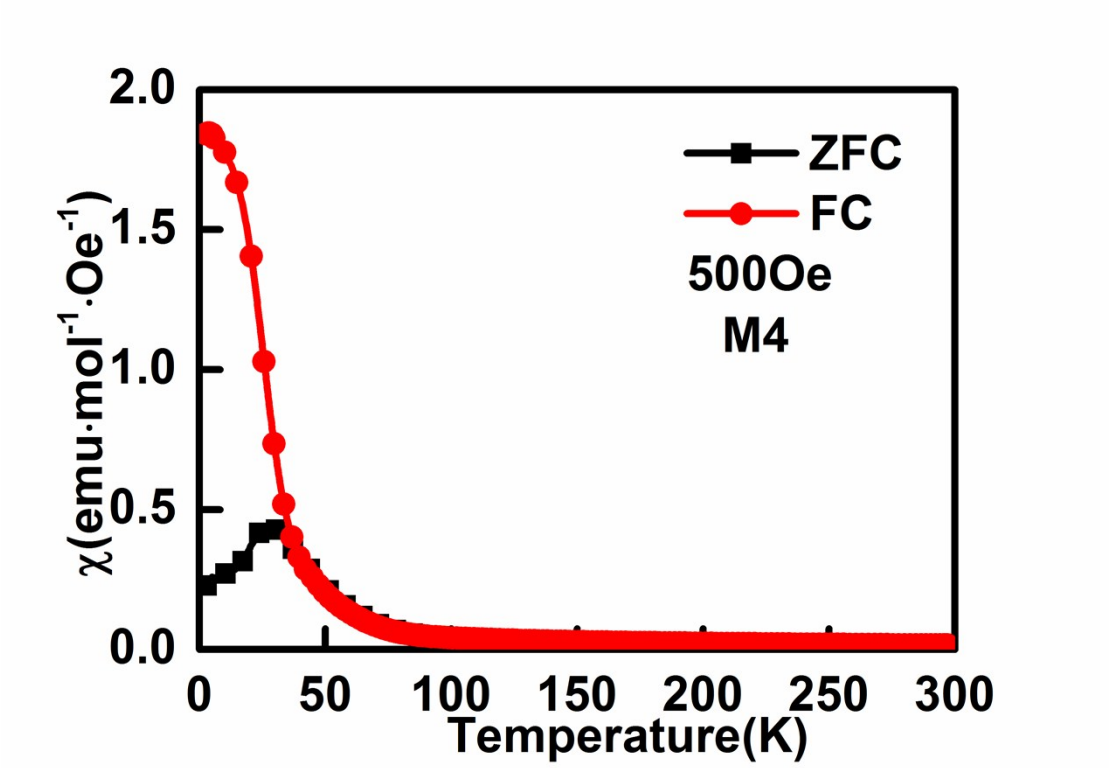

Figure S11 Temperature dependence magnetization of the samples M4 under 500 Oe in ZFC (zero field cooling) and FC modes.

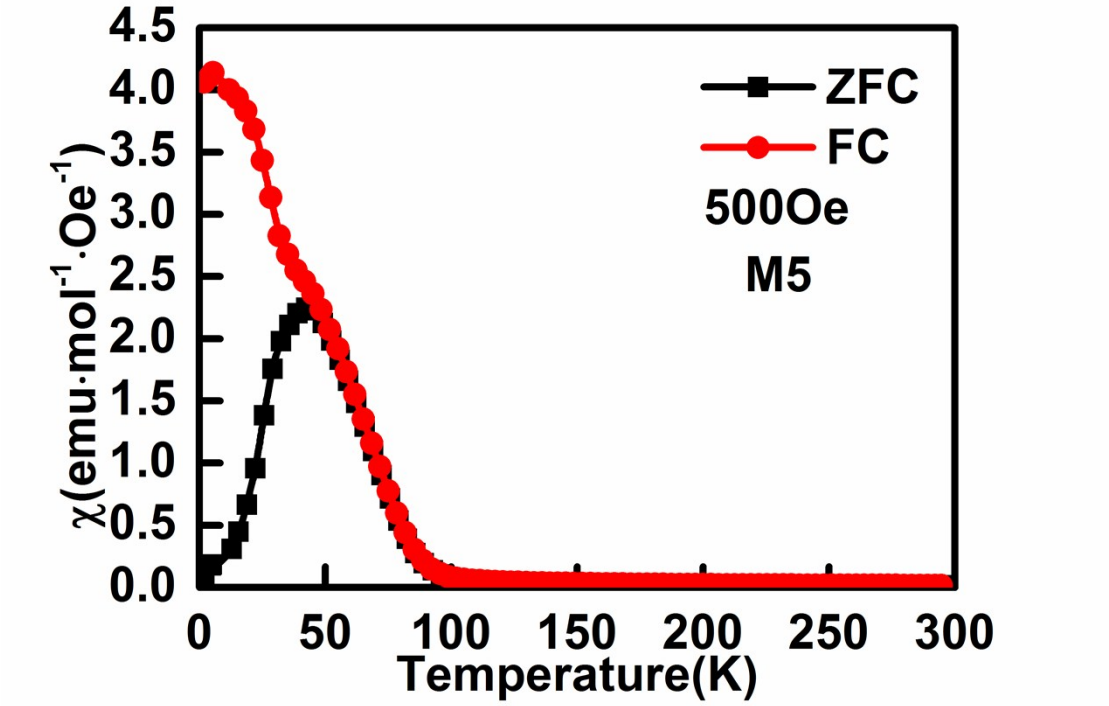

Figure S12 Temperature dependence magnetization of the samples M5 under 500 Oe in ZFC (zero field cooling) and FC modes.

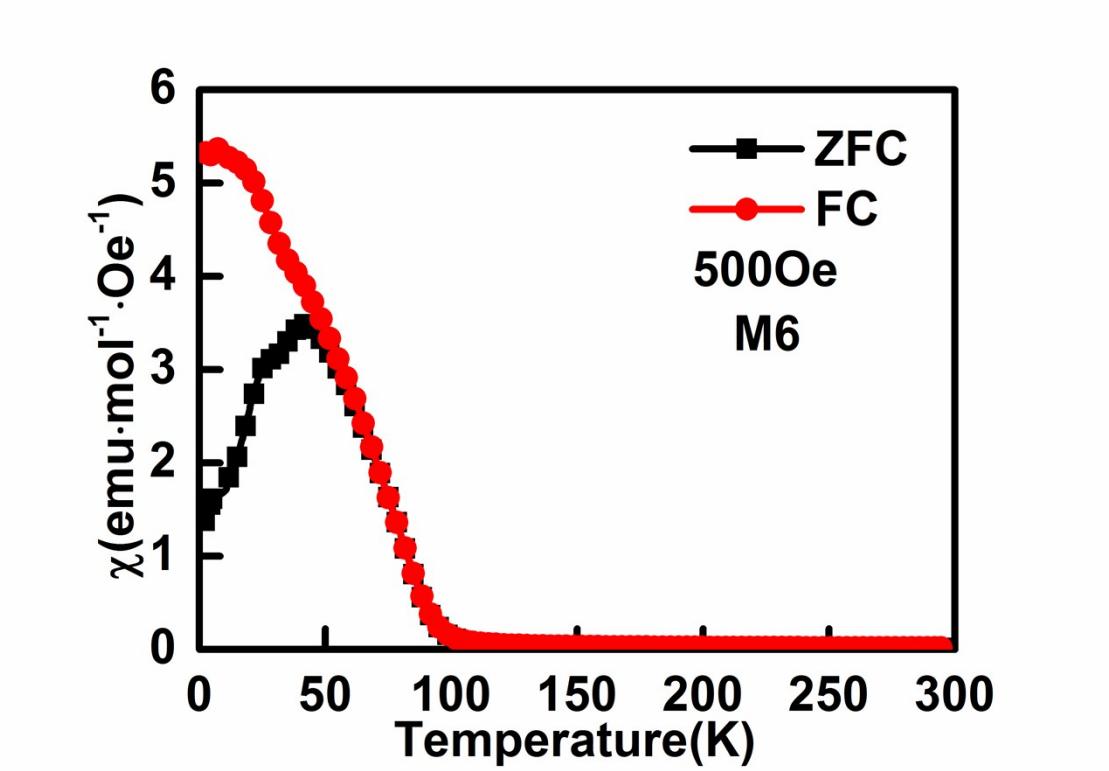

Figure S13 Temperature dependence magnetization of the samples M6 under 500 Oe in ZFC (zero field cooling) and FC modes.

3. The field dependent magnetization (M-H) curves at selected temperatures for M2 to M6.

3.1 M-H curves for M2

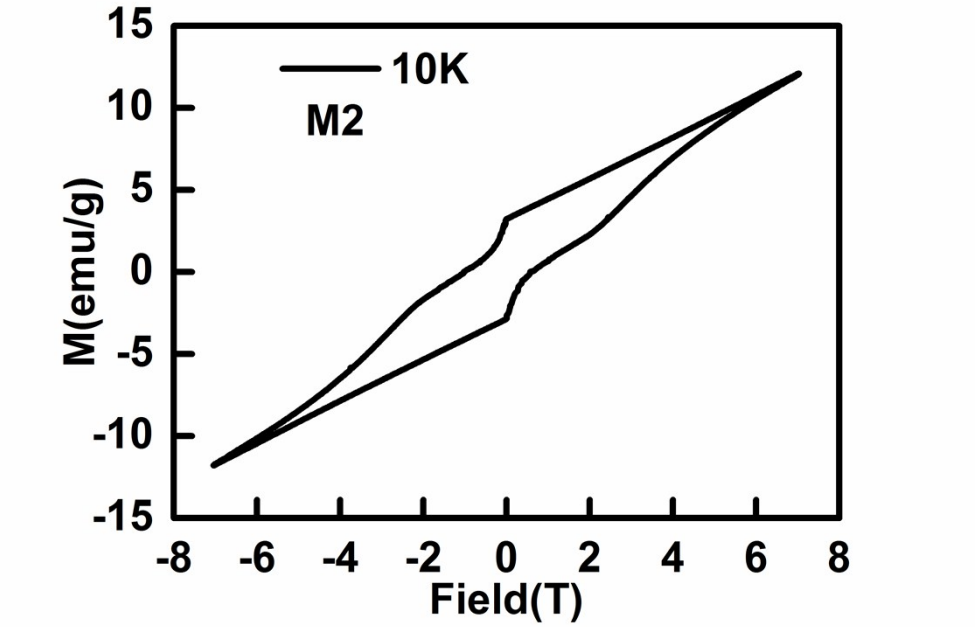

Figure S14 The field dependent magnetization (M-H) of M2 at 10K.

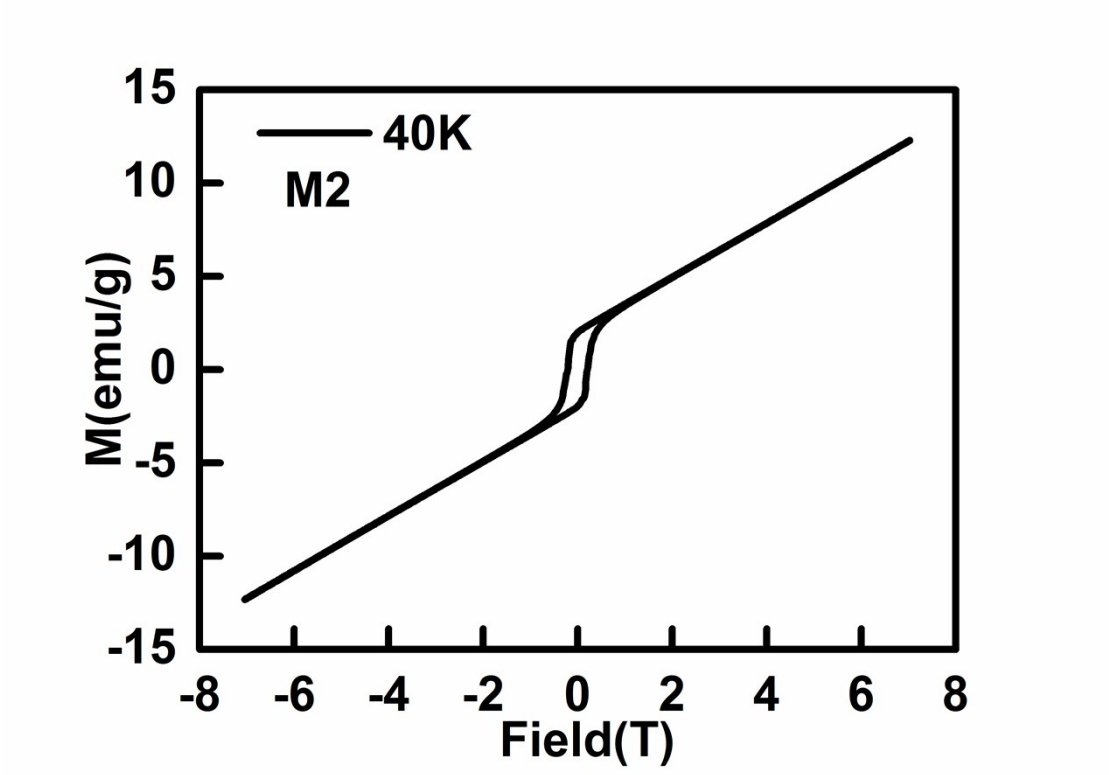

Figure S15 The field dependent magnetization (M-H) of M2 at 40K.

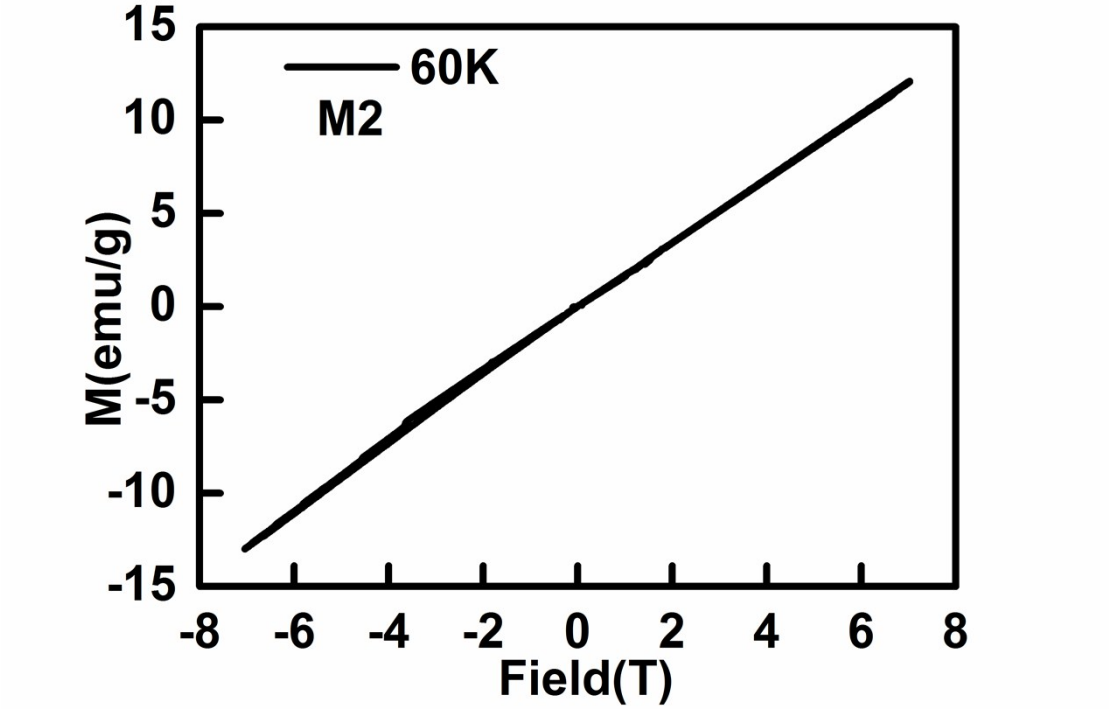

Figure S16 The field dependent magnetization (M-H) of M2 at 60K.

3.2 the M-H curves for M3

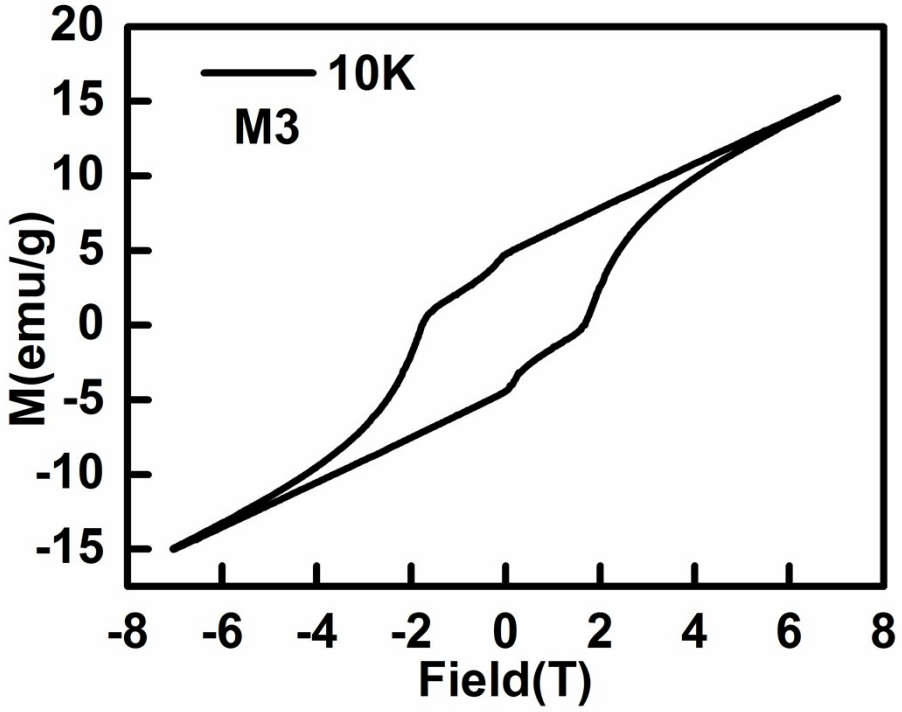

Figure S17 The field dependent magnetization (M-H) of M3 at 10K.

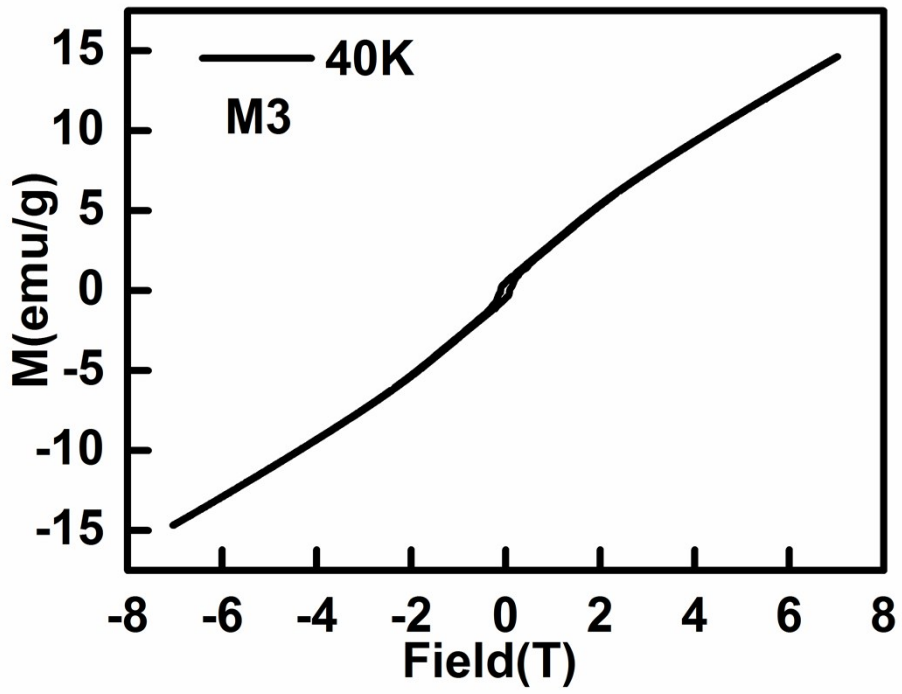

Figure S18 The field dependent magnetization (M-H) of M3 at 40K

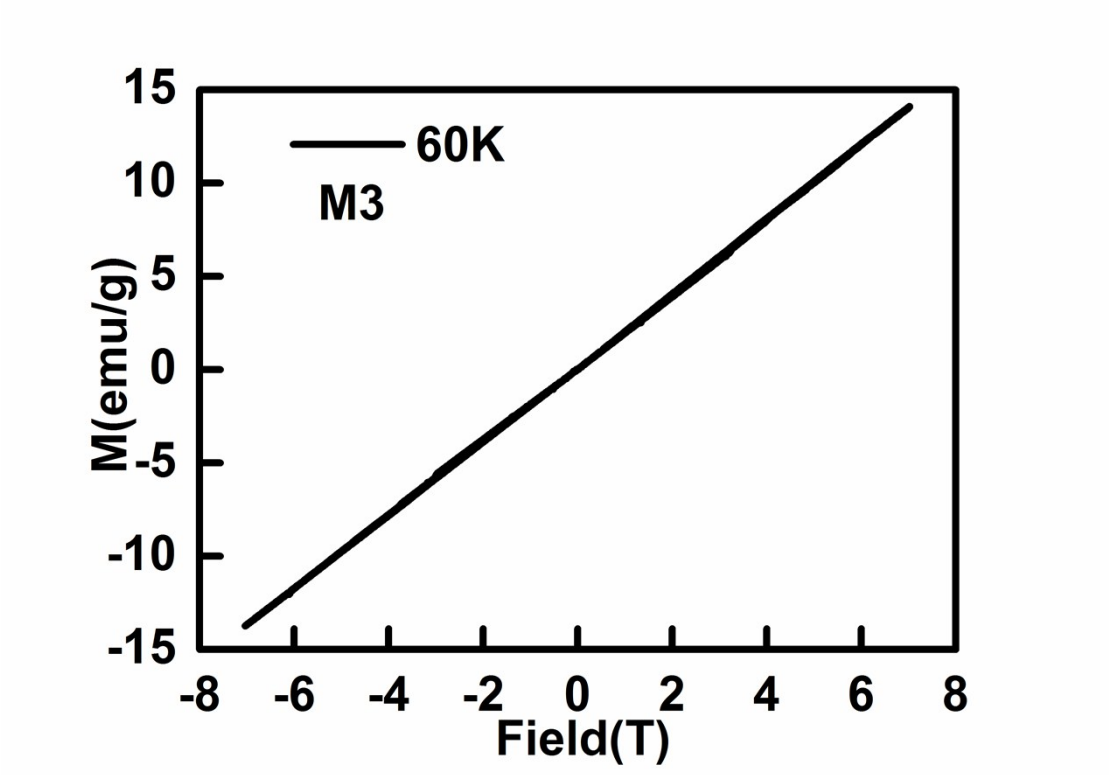

Figure S19 The field dependent magnetization (M-H) of M3 at 60K

3.3 the M-H curves for M4

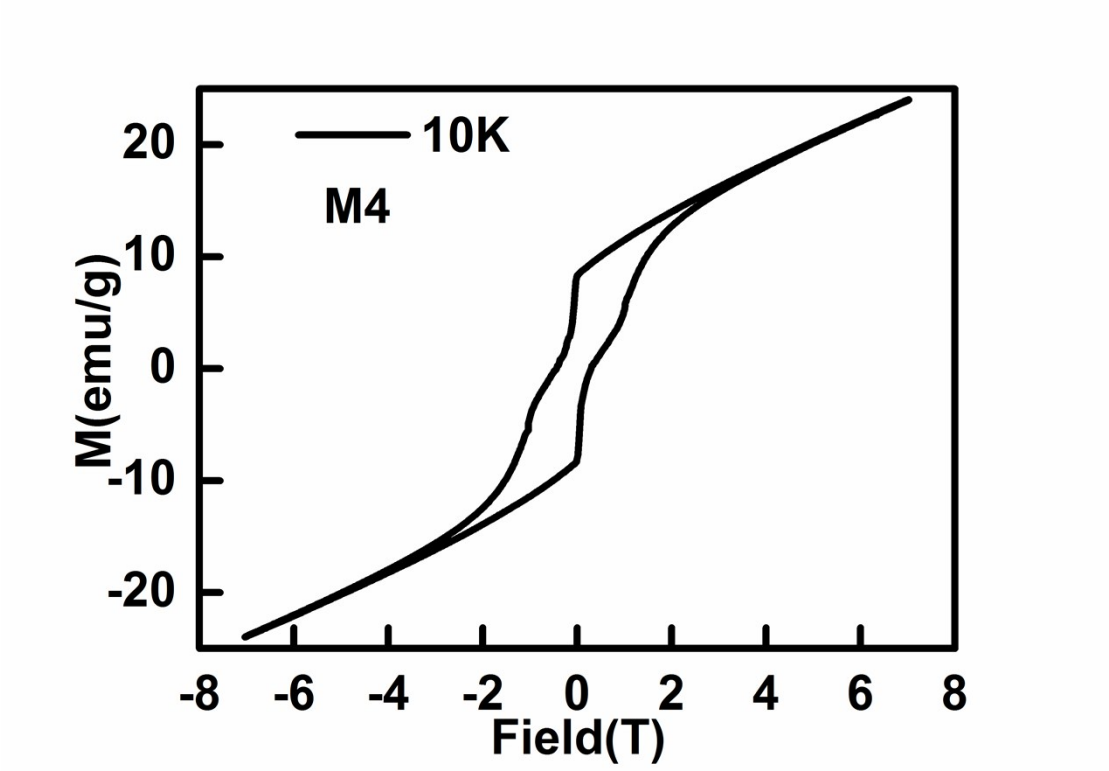

Figure S20 The field dependent magnetization (M-H) of M4 at 10K

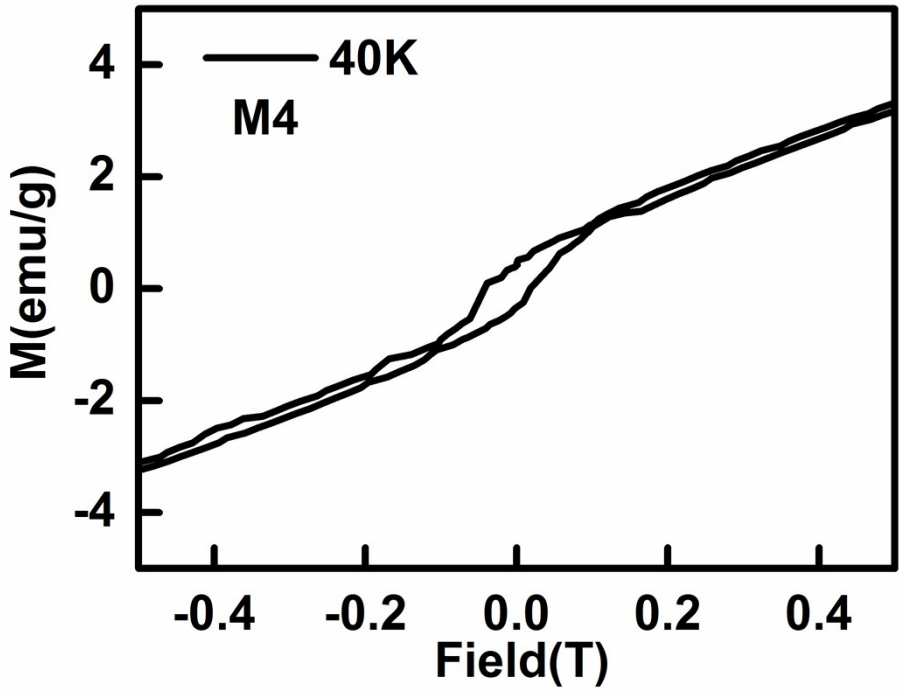

Figure S21 The field dependent magnetization (M-H) of M4 at 40K

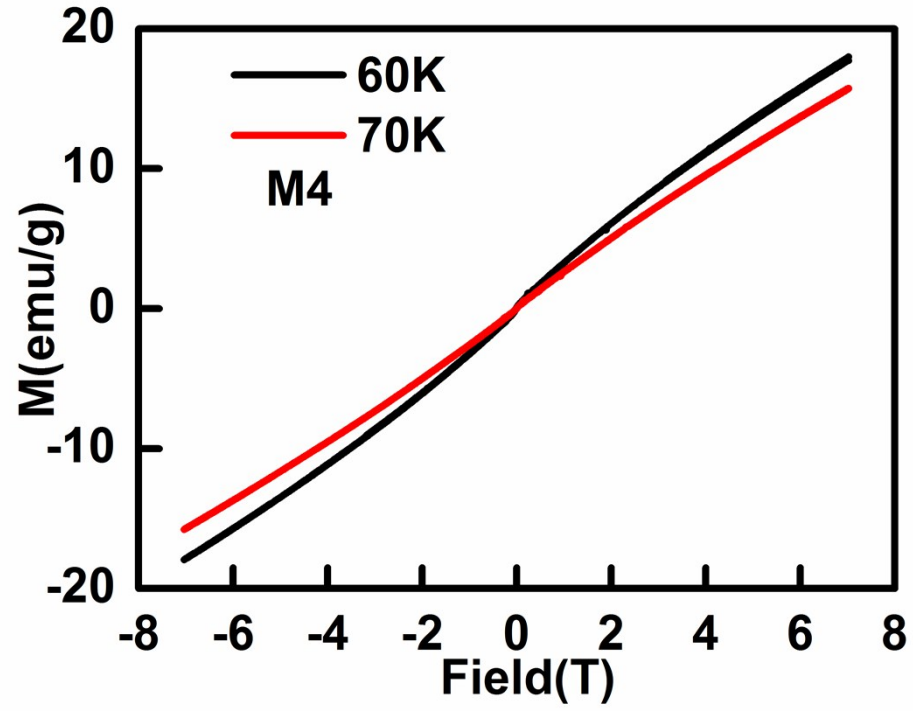

Figure S22 The field dependent magnetization (M-H) of M4 at 60K and 70K.

3.4 the M-H curves for M5

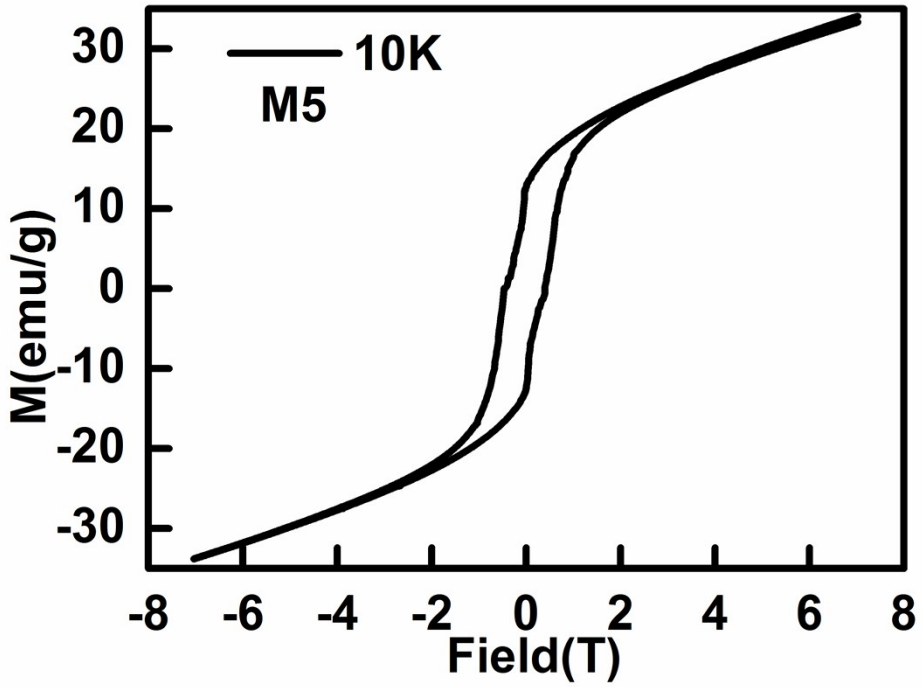

Figure S23 The field dependent magnetization (M-H) of M5 at 10K.

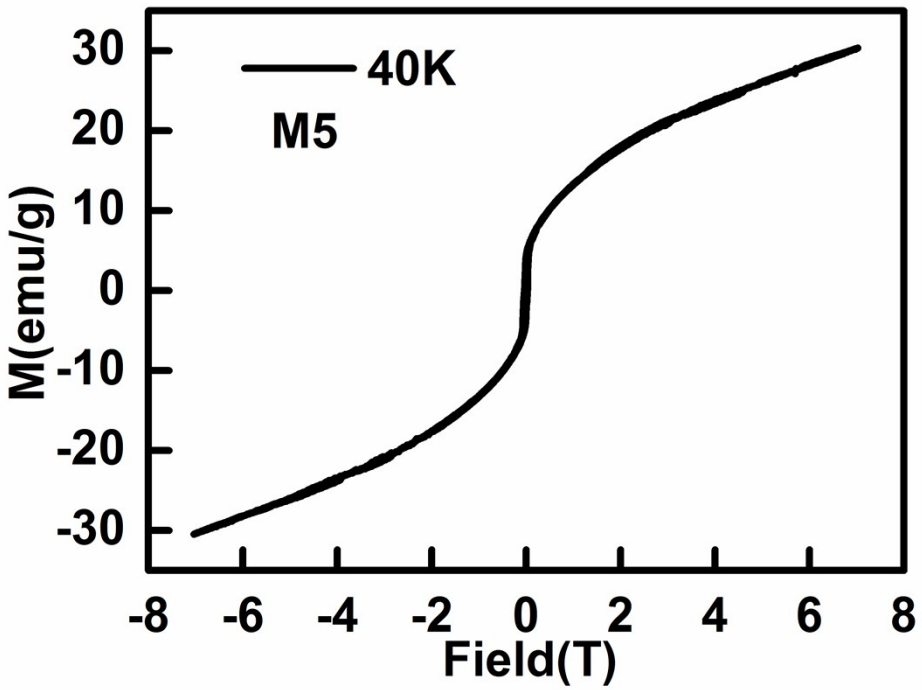

Figure S24 The field dependent magnetization (M-H) of M5 at 40K.

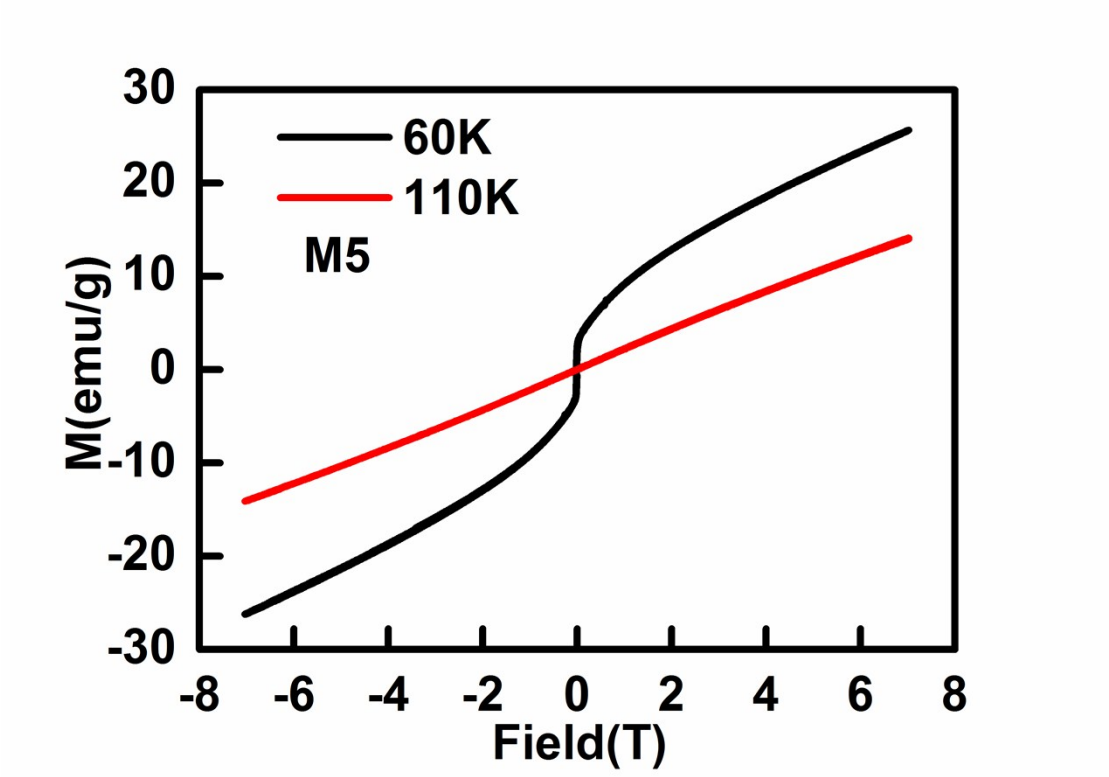

Figure S25 Field dependent magnetization (M-H) of M5 at 60K and 110K.

3.5 the M-H curves for M6

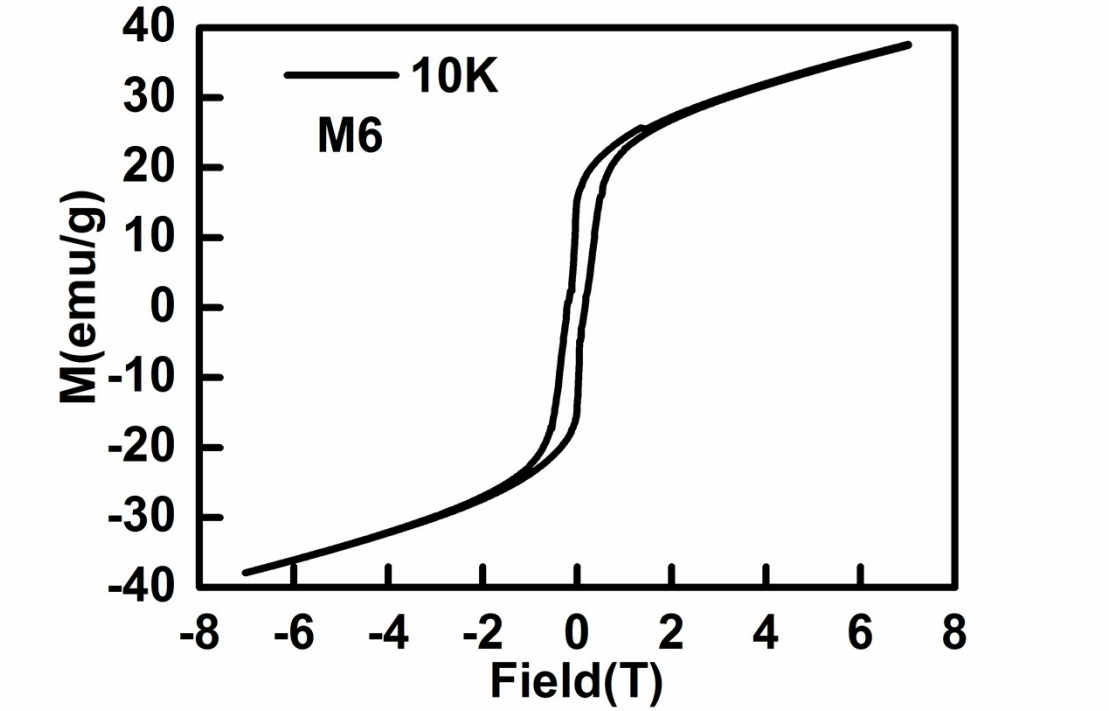

Figure S26 Field dependent magnetization (M-H) of M6 at 10K.

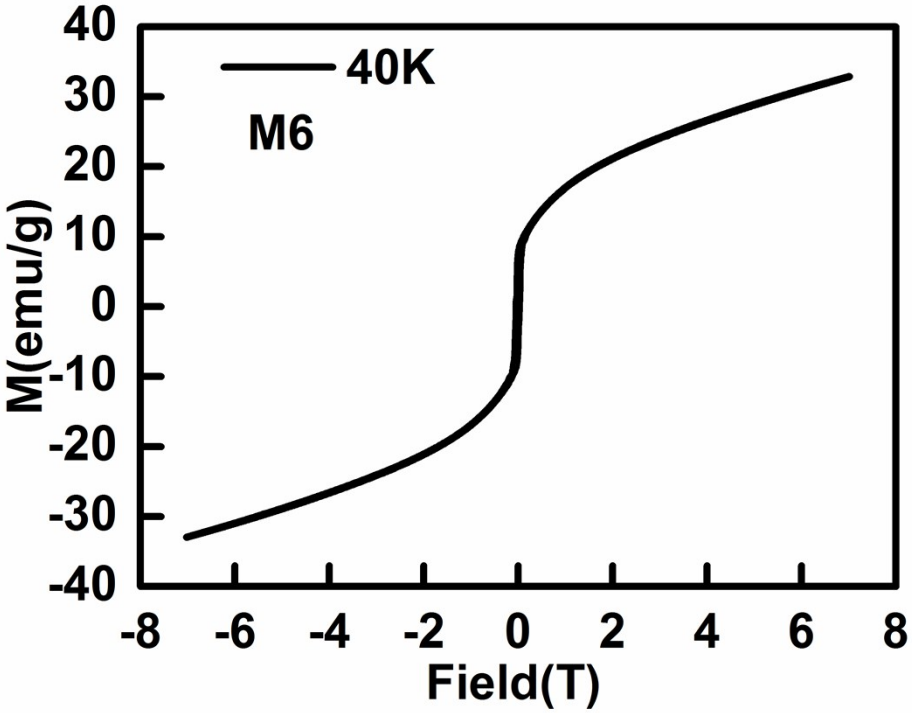

Figure S27 Field dependent magnetization (M-H) of M6 at 40K.

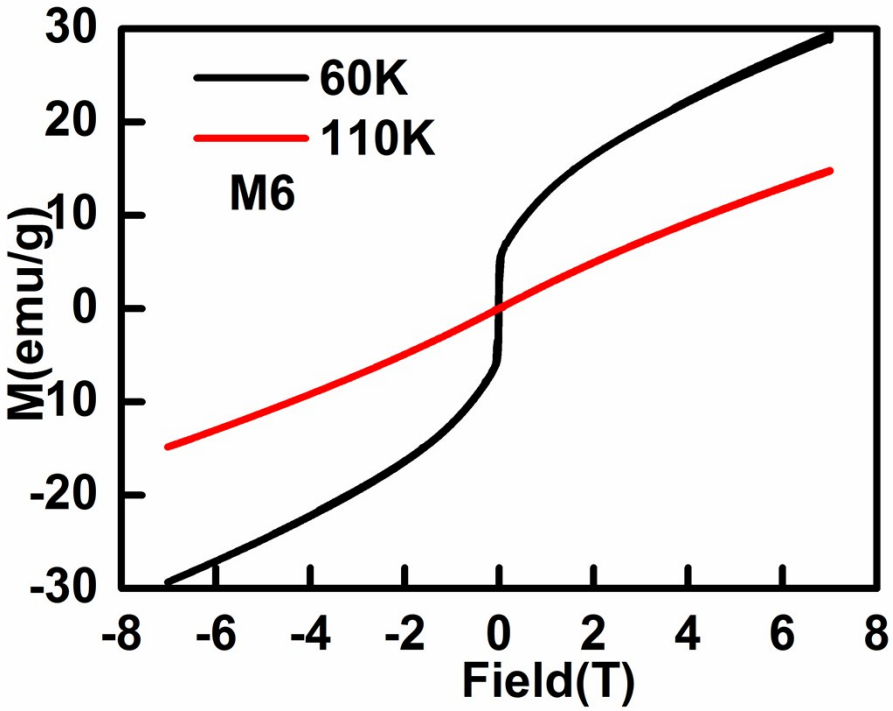

Figure S28 Field dependent magnetization (M-H) of M at 60K and 110K.

4. The X-ray diffraction data and temperature dependence magnetization of M7

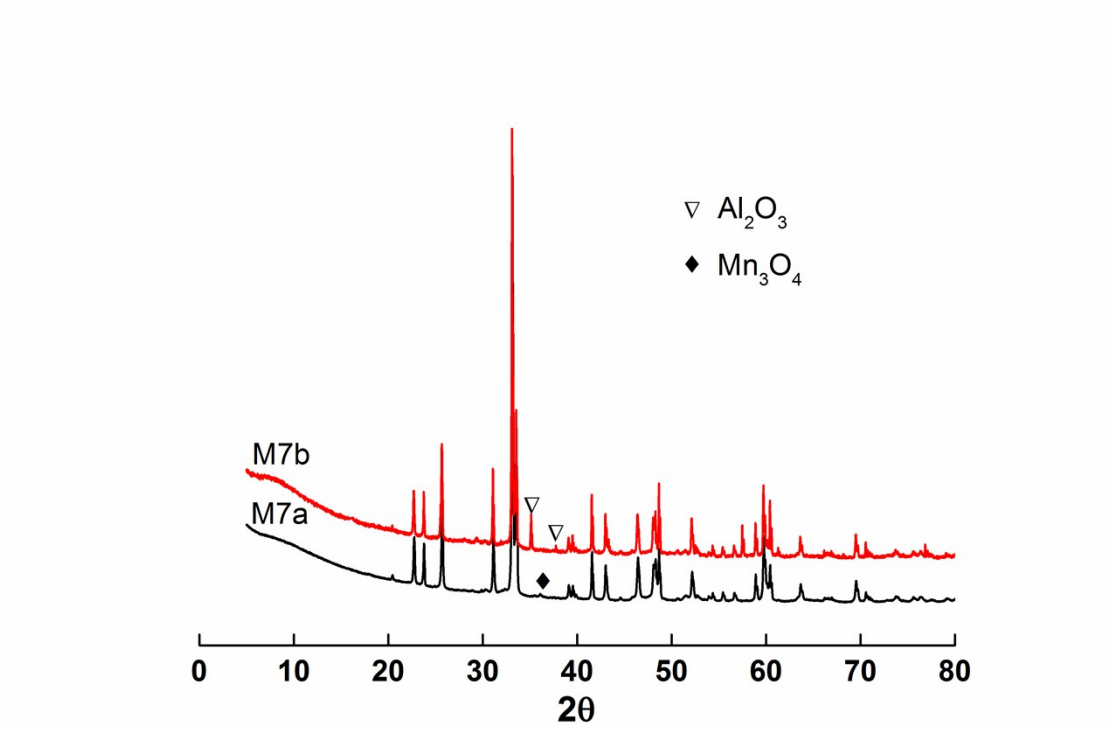

Figure S29 Powder X-ray diffraction patterns of the sample M7. The symbol 'M7a' represents the untreated sample, the symbol 'M7b' represents with treatment by KOH and KF at 200 ºC for about 24 hours, then washing them with water, and finally drying at 100 ºC. It is found that the impurity Mn_3O_4 was not detected in sample M7b. However, impurity Al_2O_3 was detected in sample M7b. The symbol ♦ stands for Mn_3O_4 and ∇ reflections for the impurity Al_2O_3. Thus, the existence of impurity Al_2O_3 have not influence on magnetization because Al^{3+} is not magnetic ion.

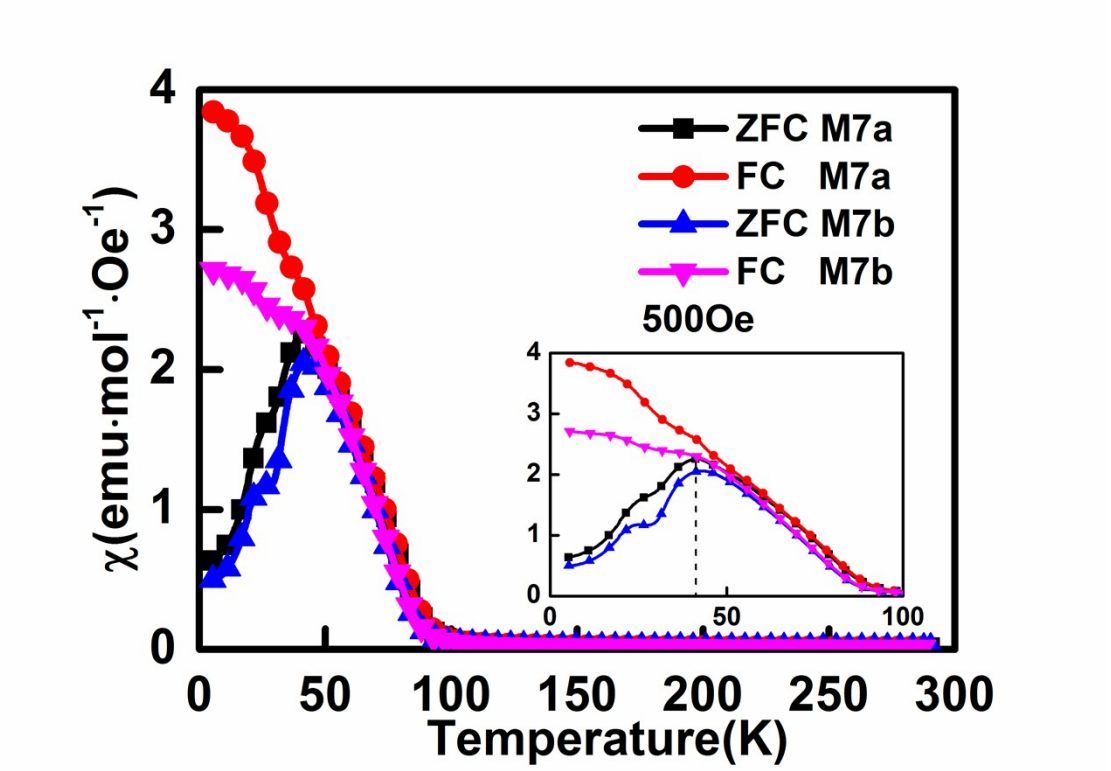

Figure S30 Temperature dependence magnetization of the sample M7 under 500 Oe in ZFC (zero field cooling) and FC modes. The symbol 'M7a' represents the untreated sample, the symbol 'M7b' represents with treatment by KOH and KF at 200 ºC for about 24 hours, then washing them with water, and finally drying at 100 ºC. It is found that the impurity Mn_3O_4 was not detected in sample M7b.